



# Engineering a Robust Photovoltaic Device with Quantum Dots and Bacteriorhodopsin

Venkatesan Renugopalakrishnan,<sup>\*,†,‡</sup> Bernardo Barbiellini,<sup>\*,§</sup> Chris King,<sup>||</sup> Michael Molinari,<sup>⊥</sup> Konstantin Mochalov,<sup>#</sup> Alyona Sukhanova,<sup>⊥,¶</sup> Igor Nabiev,<sup>⊥,¶</sup> Peter Fojan,<sup>▽</sup> Harry L. Tuller,<sup>○</sup> Michael Chin,<sup>◆</sup> Ponisseril Somasundaran,<sup>◆</sup> Esteve Padrós,<sup>¶</sup> and Seeram Ramakrishna<sup>+</sup>

<sup>†</sup>Children's Hospital, Harvard Medical School, 4 Blackfan Circle, Boston, Massachusetts 02115, United States

<sup>‡</sup>Department of Chemistry and Chemical Biology, Northeastern University, 360 Huntington Avenue, Boston, Massachusetts 02138, United States

<sup>§</sup>Department of Physics, Northeastern University, 360 Huntington Avenue, Boston, Massachusetts 02115, United States

<sup>||</sup>Department of Mathematics, Northeastern University, 567 Lake Hall, Boston, Massachusetts 02115, United States

<sup>⊥</sup>Laboratoire de Recherche en Nanosciences, LRN-EA4682, Université de Reims Champagne-Ardenne, 51100 Reims, France

<sup>#</sup>Laboratory of Nano-Bioengineering, National Research Nuclear University MEPhI "Moscow Engineering Physics Institute", 31 Kashirskoe shosse, 115409 Moscow, Russian Federation

<sup>▽</sup>Department of Physics and Nanotechnology, Aalborg University, Skjernvej 4, 9220 Aalborg Ø, Denmark

<sup>○</sup>Department of Materials Science and Engineering, MIT, 77 Massachusetts Avenue, Cambridge, Massachusetts 02139, United States

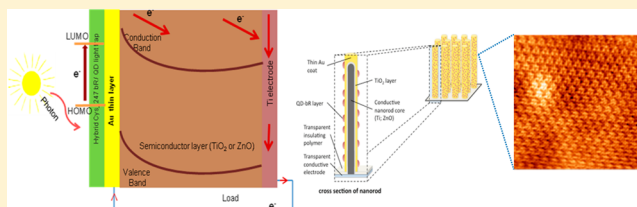
<sup>◆</sup>Langmuir Center for Colloids and Interfaces, Columbia University, 500 West 120th Street, New York, New York 10027, United States

<sup>¶</sup>Unitat de Biofísica, Departament de Bioquímica i de Biologia Molecular, Facultat de Medicina, and Centre d'Estudios en Biofísica, Universitat Autònoma de Barcelona, Barcelona, Spain

<sup>+</sup>NUS Nanoscience and Nanotechnology Initiative, National University of Singapore, 2 Engineering Drive 3, Singapore 117576, Singapore

## S Supporting Information

**ABSTRACT:** We present a route toward a radical improvement in solar cell efficiency using resonant energy transfer and sensitization of semiconductor metal oxides with a light-harvesting quantum dot (QD)/bacteriorhodopsin (bR) layer designed by protein engineering. The specific aims of our approach are (1) controlled engineering of highly ordered bR/QD complexes; (2) replacement of the liquid electrolyte by a thin layer of gold; (3) highly oriented deposition of bR/QD complexes on a gold layer; and (4) use of the Forster resonance energy transfer coupling between bR and QDs to achieve an efficient absorbing layer for dye-sensitized solar cells. This proposed approach is based on the unique optical characteristics of QDs, on the photovoltaic properties of bR, and on state-of-the-art nanobioengineering technologies. It permits spatial and optical coupling together with control of hybrid material components on the bionanoscale. This method paves the way to the development of the solid-state photovoltaic device with the efficiency increased to practical levels.



## 1. INTRODUCTION

At the heart of every photovoltaic device is a mechanism for photon-to-electrical transduction. Ideally, the device should capture light across a broad spectrum and efficiently transfer the energy of photons to the electrons. Current dye-sensitized solar cell (DSSC) designs<sup>1–3</sup> have achieved efficiencies of over 10% but make use of expensive, toxic compounds (e.g., Ru-based dyes) and comprise a reactive liquid electrolyte, leading to potential sealing and aging/degradation problems of the solar panels. In 2003, McFarland and Tang proposed a design shown in Figure 1, which removes the need for the liquid electrolyte,<sup>4</sup> although an inefficient absorbing layer remained as

a component of their system, keeping the efficiency at the 1% level.

Photosynthesis involves the most advanced and efficient system nature has crafted to convert solar energy into an electrical potential and into chemical compounds for energy storage. Biosolar and biofuel cells represent the emerging

**Special Issue:** Michael Grätzel Festschrift

**Received:** December 27, 2013

**Revised:** May 14, 2014

**Published:** May 16, 2014

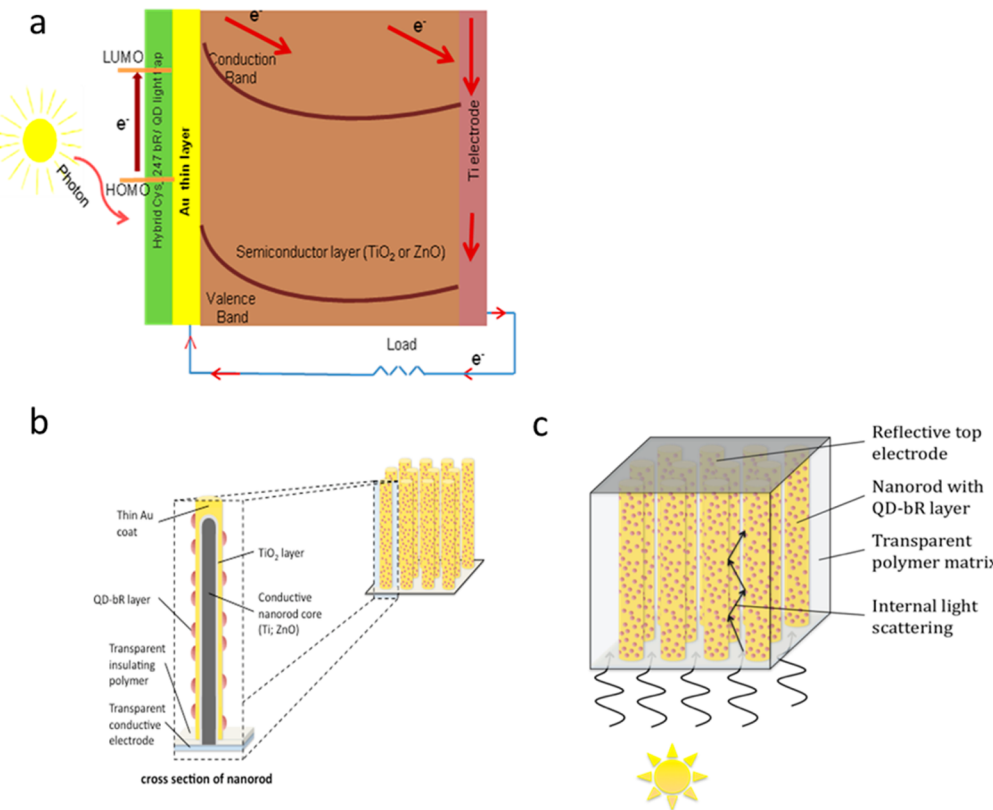


**Figure 1.** (a) Planar structure of the solid-state photovoltaic device. (b) Illustration of a nanowire array showing the conductive core, covered, respectively, by  $\text{TiO}_2$  (or  $\text{ZnO}$ ) semiconductor metal oxides, Au, and QD-bR dye layers. Panel c illustrates how the nanowire array can be packaged to include a lower transparent electrode, a transparent polymer matrix to provide mechanical stability and flexibility, and a top reflective electrode. The polymer matrix can include particles with index of refraction differing from the matrix to further enhance internal reflections.

frontier in the development of green energy sources. In recent years, Thavasi et al.<sup>5</sup> reported several advances for the feasibility of bacteriorhodopsin (bR) as biophotosensitizer in excitonic solar cells. The protein bR has been the focus of development for technological applications in information storage, excitonic solar cells, and sensors.<sup>5–7</sup> This integral membrane protein from purple membranes (PMs) of bacteria *Halobacterium salinarum* shows a high yield of expression, high thermal and chemical stability, and good charge separation on photon absorption. The intrinsic stability of bR is unusually high compared with other proteins found in archaeabacteria. Essentially, the capability of bR to complete photoconversions with no loss of its photonic properties is far beyond the capacity of any synthetic material. These intrinsic properties have made this protein an excellent candidate with attractive physical functions, which can be used in nanoscale devices. While bR acts as a light-driven proton pump during charge separation on photon absorption, electron ejection occurs concurrently. Because of the later property of bR, it is logical to leverage its application in excitonic solar cells. Its light-induced electrical signal possesses a very fast rise time on the order of picoseconds, and its quantum efficiency is high ( $\sim 0.64$ ).

Protein engineering has created an extensive library of bR mutants with each mutant designed for specific technological application. There are at least two classes of bR mutants suited for solar cell application. One class of such mutants was developed to facilitate charge separation through mutating Glu residues with side chain's negative charges to Gln residues. Four negatively charged glutamate side chains, Glu9, Glu74, Glu194, and Glu204<sup>8</sup> are located in the extracellular (EC) region of bR.<sup>9</sup>

This has led to a bR triple mutant E9Q/E194Q/E204Q bR, which has been used in the construction of excitonic solar cells.<sup>5</sup> Furthermore, it was found to transfer electrons from the redox electrolyte to the anode better than wild-type bR, thus enabling it to be used as a photosensitizer. One of the specific requirements for using naturally occurring organic molecules in technological devices is their structural and functional stability in a wide range of temperature (up to  $80\text{ }^\circ\text{C}$ ) and pH. Because a wild-type bR lacks Cys residue often necessary for PM immobilization and orientation, the mutants with the Cys-residues in positions 3, 36, and 247 of bR amino acid sequence were engineered. At least three Cys-bR mutants (T247Cys bR, D36Cys bR, and Q3Cys bR) appear to be promising for excitonic solar cells because Cys residues are amenable to covalent linking to Au through their sulphydryl group. Gold plays an important role in facilitating ballistic electron transport through interfaces.<sup>10</sup>

While there are many different materials<sup>11</sup> and configurations designed to achieve the DSSC effect, the biosensitized solar cell (BSSC)<sup>5,12,13</sup> has an advantage of the use of low-cost and environmental friendly biomaterials able to enhance the energy-transfer efficiency.<sup>14</sup>

A new BSSC design consists of two key components, which implement the energy-transfer step, namely, a hybrid material engineered from protein bR and quantum dots (QDs) to absorb and trap the photon energy<sup>15–18</sup> and a thin layer of gold (Au) to produce the ballistic electrons and recycle the retinol fragment in bR. The transfer of light energy absorbed by QDs to bR occurs first via an efficient Forster resonance energy transfer (FRET)<sup>19</sup> and further, from bR-QD to Au, via a

nonradiative “Auger-mediated de-excitation” (AMD) in the Au layer.<sup>20,21</sup>

The enhanced thermal stability of bR and its mutants, accomplished by rational site-directed mutations,<sup>22</sup> is yet another transformative element of the BSSC.

The operation of these three key transformative BSSC paradigms holds great promise for construction of robust and efficient electrolyte free solid-state photovoltaic devices illustrated in Figure 1. In this device, photons hitting the layer of dye molecules cause excitation, which results in electrons being injected into the gold layer. The electrons can move in a ballistic way across the thin gold film and over the Schottky barrier into the conduction band of the TiO<sub>2</sub> layer. If instead the electrons lose energy in the gold layer (becoming “thermalized”), they are no longer energetic enough to cross the Schottky barrier. An advantage of this device is that the excited bR/QD layer is automatically regenerated by electron donation from the gold film. For the sake of simplicity, initial trials toward this effort are with planar structures similar to that of McFarland and Tang (Au/TiO<sub>2</sub>/back contact). These exploratory investigations can be then followed by the fabrication of a nanowire array composed of a Au-coated semiconducting metal oxide (TiO<sub>2</sub> or ZnO), coated in turn with the hybrid QD-bR proteins; see the bottom of Figure 1. This more complex morphology will serve to markedly increase the active area, significantly reduce losses due to reflectivity, given that photons penetrating into the mesoporous or nanowire forest will exhibit multiple reflections within the array, and ultimately be absorbed, as demonstrated recently by Atwater and coworkers for Si nanowire arrays.<sup>23</sup> This arrangement also offers more tunable mechanical properties. In practice, anodization of Ti foils can be used to prepare the TiO<sub>2</sub> nanotubes,<sup>24</sup> while Au films can be applied to the oxide nanowires by either thermal evaporation or electrodeposition.<sup>25</sup>

A roadmap toward a radical improvement in solar cell efficiency using the recent innovations in the BSSC paradigm previously introduced is presented in this paper. Section 2 summarizes first-principles computational methods to predict the efficiency of the sensitized solar cells. Section 3 introduces the new absorbing hybrid layer composed with QDs and bR, whereas the technical details to prepare the absorbing layer and advanced approaches to characterization of the functional and structural properties of this layer are presented in Sections 4 and 5, respectively. The conclusion, outlook, and perspectives of the creation of solid-state photovoltaic device with efficiency increased to practical levels are given in Section 6.

## 2. QUANTUM DESIGN OF SENSITIZED SOLAR CELL

Quantum calculations are useful here because they can deal with electronic effects, electron delocalization, charge-transfer, and other phenomena, which are otherwise difficult or impossible to treat at the level of classical mechanics. Ab initio (or first-principles) calculations are an attempt to solve the Schrödinger equation, making approximations as needed. The first approximation (the Born–Oppenheimer approximation) is that the nuclei do not move much, relative to the electrons. Thus, the nuclei are fixed in space, and the calculation is to determine the distribution of electrons around the nuclei, orbital by orbital. Standard ab initio approaches are density functional theory (DFT) and quantum Monte Carlo (QMC). The DFT deals with the electron density, while the QMC directly uses the many-body wave function of the system. Extensive DFT and time-dependent DFT study of the DSSC

sensitizer (QD or dye) have been performed, investigating various effects on the electronic structure and optical properties of the system.<sup>26</sup> The highly precise QMC methodology developed to study many-body wave functions is also used to test the DFT results.<sup>27</sup> Thus, first-principles simulations are used to extract the electronic characteristics needed to design new photovoltaic cells. The calculated wave functions and energy levels yield rates and efficiencies of various photovoltaic processes. For example, we have performed a DFT calculation for the retinal protonated Schiff base (RPSB) chromophore of bR using the 6-31G\*\* basis set and the B3LYP exchange-correlation potential.<sup>28</sup> The energy  $E_g$  between the highest occupied molecular orbital (HOMO) and the lowest unoccupied molecular orbital (LUMO) of retinal in bR is ~2.6 eV. At the Hartree–Fock level, this energy is 7.9 eV; therefore, correlation effects play an important role on the gap size. The chromophore can be stabilized in the bR by the HOMO–LUMO interaction with the protein environment. As a result, the HOMO–LUMO gap of the chromophore is expected to shrink inside the tight bR protein pocket. These results can be checked with X-ray photoemission spectroscopy (XPS), X-ray absorption spectroscopy (XAS), and ultraviolet photoemission spectroscopy (UPS).<sup>28</sup>

In general, the ultimate efficiency for solar cells can be written as  $F_0 = E_g Q_s / P_{in}$ , where  $E_g$  is here the energy needed to produce one electron–hole pair,  $Q_s$  is the number of photons per unit of time with energy higher than  $E_g$ , and  $P_{in}$  is the total incident power. In a typical solar cell, however, the efficiency  $F$  is a fraction of  $F_0$  given by  $F = t_s r m F_0$  (Shpaisman et al., 2008). Here  $t_s$  is the probability to produce an electron–hole pair from a photon with energy  $E_g$  (or higher). The probability  $t_s$  depends on the size of the active absorption layer; the quantity  $r = V_{oc} / E_g$  is the ratio of the open-circuit voltage  $V_{oc}$  and the band gap; and  $m$  is the impedance matching factor depending on internal cell resistances. To arrive at a more efficient system, we must simultaneously optimize all parameters ( $F_0$ ,  $t_s$ ,  $r$ , and  $m$ ). Ideally, the ratio  $r$  should be close to one if the energy losses are minimized in the charge-separation process.

The electron and positive hole once formed must be separated to avoid rapid charge recombination between the electron and hole. The basic idea is to move electrons from one side of a compound to the other side as quickly and as efficiently as possible so that the positive and negative charges become spatially remote. The AMD<sup>20,21</sup> shown in Figure 2 is an efficient quantum mechanism to separate the charge by transferring the energy from the dye (donor) to the substrate (acceptor) through a single step, and it is similar to a photoelectric effect involving virtual photons. Because the photons are virtual, the selection rules do not apply; therefore,

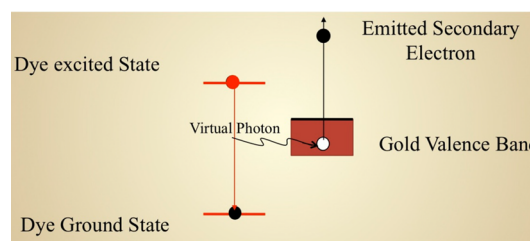


**Figure 2.** Schematics of the Auger-mediated de-excitation mechanism to separate the charge by transferring the energy from the dye (donor) to the substrate (acceptor) through a single step.

the rates are usually large and thus the injection time is short. In the energy band structure of the device shown in Figure 1,  $E_F$  is the Fermi level (in the dark) and  $E_{qF}$  is the quasi-Fermi level under illumination. Thus, we have  $V_{oc} = E_{qF} - E_F$  and the parameter  $r$  can then be calculated from first-principles simulations.

Positron annihilation spectroscopy combined with first-principles simulations has already revealed unique information regarding the surface of nanostructured materials forming the McFarland–Tang device of Figure 1.<sup>29–31</sup> Therefore, further simulations validated by several experiments can illuminate routes toward 15% efficiency for DSCCs and BSSCs.

### 3. ACTIVE QD/bR ABSORPTION LAYER WITH CONTROLLED FORSTER RESONANCE ENERGY TRANSFER EFFICIENCY

In this section, we seek to develop an absorbing layer to funnel the energy flow by a combination of electronic, optical, and excitonic means.<sup>32</sup> The goal of efficient energy transfer can be achieved by designing a hybrid layer composed of QDs and bR. The mechanism for this transfer in the QD/bR layer relies on the near-field resonance of electric dipoles and is generally known as FRET. In its simplest formulation, FRET is the quantum version of a classical resonance phenomenon, whereby oscillating electric dipoles exchange energy through their mutual electric fields.

In a recent work,<sup>19</sup> we have revisited the analysis of the rate and efficiency of FRET in the context of a donor and an acceptor species with comparable electronic energy gaps. In our model, the coupling elements QD and bR are governed by point-dipole/point-dipole coupling. Our approach uses density matrix formalism linking Perrin's coherent FRET calculations (performed 14 years before Forster's work) to the standard incoherent hopping dynamics derived by Forster from Fermi's golden rule. To introduce the vibronic coupling in bR, we have proceeded by analogy to the derivation of the line shape of a resonance. We have used the fact that a resonance is a perturbation of an embedded eigenvalue in continuous spectrum. Thus, we assume that the probability amplitude of the bR exciton in the diagonal energy representation is given as the square root of a Lorentzian. The width  $\gamma$  of this Lorentzian characterizes the vibronic coupling and determines the lifetime of the exciton. Thus, in the present scheme, the vibronic coupling always produces decoherence. Our model applies in situations where the donor molecule (QD) is rigid, with weak coupling between its electronic and vibronic states, while the acceptor (bR) has strong electronic-vibronic coupling in its excited state. In this situation, the model is exactly solvable and thus allows a comparison with the incoherent limit derived by Forster and others. In particular, we have derived exact formulas for FRET efficiency and the Forster radius, and we compare these with the well-known Forster formulas. Furthermore, the model is fully quantum mechanical and predicts coherent oscillations between donor and acceptor when the parameter  $\gamma$  is small. An important goal of the first-principles simulations is to calculate parameters for our exact model that can predict the Forster radius in the engineered protein bR and semiconductor QD hybrid material.<sup>17,18</sup> This material is important because it might provide an efficient active absorption layer for a new type of biosolar cell. In fact, our recent experimental work<sup>18</sup> has shown that the QD/bR system can provide FRET efficiencies substantially exceeding the values predicted by the classical FRET theory formulated by Forster.

The use of QDs as photoabsorbers is well studied, and several advantages are clear. The most prominent is the ability to tune the absorption spectrum by modifying the size and morphology of the QD. However, current photovoltaic devices using QDs suffer from low efficiency, which is partially related to the re-emission by the QDs of the absorbed light through fluorescence, resulting in photocurrent losses. If the QD absorption layer is replaced by a hybrid layer composed of QDs and bR molecules, the fluorescence emission of QDs can be selected to ensure maximal spectral overlap with bR absorption. In this architecture, the complexes are engineered in such a way that each QD is coupled to one bR trimer, thus providing both spatial and optical bR/QD coupling. This design ensures minimal spatial distance between donor (QD) and acceptor (bR) and maximal spectral overlap between donor fluorescence and acceptor absorption: two conditions guaranteeing maximal efficiency of resonance energy transfer in bR/QD hybrid material.<sup>16–18</sup> This results from the optical coupling between the QD and bR, which converts re-emission of light from the QD within its energy nonradiative transfer to bR, and thereby increases the amount of trapped incident energy available for conversion to photocurrent. As previously mentioned, the mechanism for this coupling is based on FRET, which provides an efficient avenue for energy transfer between molecules separated by distances of up to 15 nm.<sup>18</sup> In this case, a correct treatment of *quantum coherence* plays a key role in the optimization of this process.<sup>19</sup> Furthermore, bR is known as an efficient trap for light energy, effectively locking the energy in place by a conformational distortion of the retinal molecule due to *cis*–*trans* isomerization. Thus, the QD acts as the antenna and the bR acts as the storage device. Our previous studies<sup>3</sup> have demonstrated that bR alone can play the role of the dye in an initial version of the BSCC. Another previous work<sup>12</sup> estimated that the maximal theoretical efficiency for a bR cell could reach 25%, which is comparable to silicon. Moreover, this work also reported that the average specific power for bR is 2103 W/kg compared with 32 W/kg in Si. Such a large number suggests the possibility to store a large amount of excitons in bR, making the absorbing layer very efficient. The QDs can be tailored to re-emit the absorbed light at the wavelength that is most efficiently absorbed by bR, thus increasing the quantity of solar energy captured. Therefore, when QDs are attached to bR, one expects a substantial increase in the bR/QD photovoltage over that of just bR.<sup>17,18</sup>

The bR within its natural PM can be visualized with an atomic force microscope (AFM), as illustrated in Figure 3, where the PM was deposited on a mica. Highly oriented monolayers of bR in PM form<sup>33</sup> can be obtained by the reaction of bR-Q3C with a gold surface through the covalent coupling of Cys-residues introduced in the amino-acid sequences of the bR mutants (as previously explained). The FRET coupling between QDs and bR can be controlled by varying the linker between a bR trimer and a QD receiving the light. AFM imaging revealed correlation between the known surface charge of QDs and their ordering degree on the surface of PM.<sup>17</sup> The most FRET-efficient QD-PM complexes have the highest level of QDs ordering, and their assembling design may be further optimized to engineer hybrid materials with advanced biophotonic and photovoltaic properties.<sup>17</sup>

An increase in the QD/bR ratio used for assembling of QD-bR hybrid material leads to disappearance of the regular ordering of QD on the surface of the PMs, as shown in Figure 3d. The data presume specific binding of QD with the bR

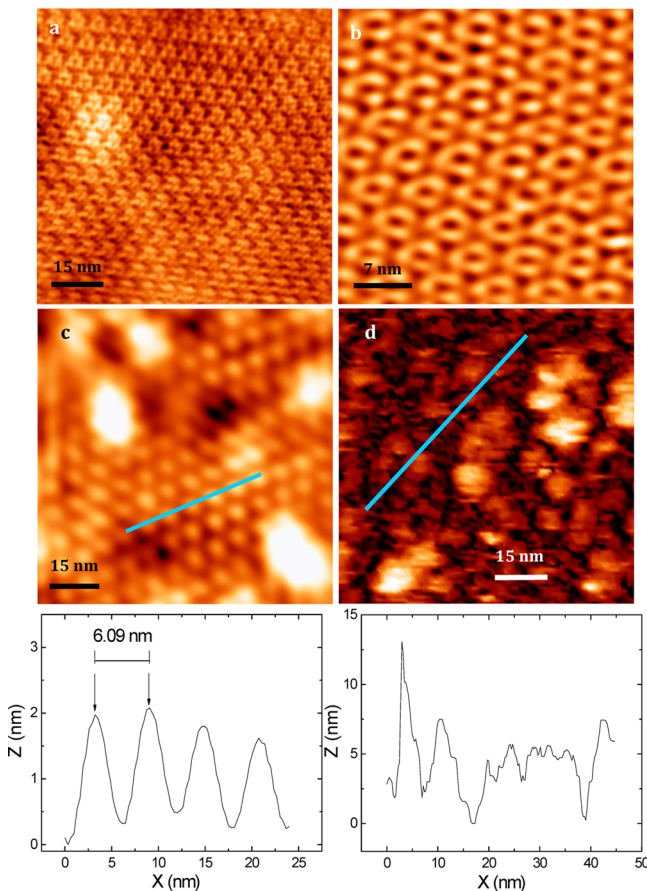


**Figure 3.** AFM images of bR within its natural PM (a,b) and the same images for the assemblies of PM with QDs (c,d). Panels a and b show an AFM image of bR trimers forming hexagonal crystal lattice with a period of  $\sim 6.2$  nm. Panel c shows that the disposition of quasi-epitaxial QDs on the surface of PMs corresponds to the hexagonal crystal lattice of bR with a period constant of 6.1 nm, nearly the same as for bR trimers.

trimers on the surface of the PM at the approximately one-to-two QD/bR molar ratios, followed by the formation of nonregular and nonordered multilayered QD-structures upon an increase in the QD/bR molar ratios.

The bottom parts of the Figure 3c,d show the AFM-profiles scanned along some parts of the blue lines indicated on the AFM-images in the corresponding middle panels. The period of QD organization on the PM upon assembling of hybrid material at the low (one-to-two) QD/bR ratio (6.09 nm, Figure 3c) corresponds well to the period of bR trimers organization within the PM (6.2 nm).

#### 4. EXPERIMENTAL PROTOCOLS: PROTEIN ENGINEERING OF Cys247 bR AND COVALENT ATTACHMENT OF Au TO CYS SULFHYDRYL GROUPS

The bR mutant T247C *bop* gene was obtained as described by Sanz et al.<sup>34</sup> substituting the shuttle vector pXL by the site-specific integration vector pEF191 (kindly provided by Dr. Mathias Lubben). The mutated gene was transformed into the bR-deficient strain MPK409 and the clones were selected.<sup>35</sup> The mutation was confirmed from *H. salinarum* transformants by sequencing the *bop* gene from isolated DNA. Purple

membrane was grown and purified following the standard procedure.<sup>36</sup>

Cys247 bR at a concentration of 6.67 g/L was diluted 10 times in suspension buffer (150 mM KCl, 10 mM Tris-HCl, pH 8.2) to a final absorbance of 0.2 to 0.3 at 570 nm. We mixed 0.5 mL of this diluted bR solution in suspension buffer with 250  $\mu$ L of incubation buffer (300 mM KCl, 10 mM Tris-HCl, pH 7.82), and this mixture was placed on the glass substrate coated with gold (Au) and incubated for 6 h for bR attachment. The container was kept in the dark during the attachment process, and the process was carried out at room temperature. After 6 h, the substrate was rinsed with incubation buffer several times, followed by drying at room temperature in the dark for 5 to 6 h and always kept under dark conditions.

After the rinsing, visual attachment did show pink and purple spots on the Au substrate. Demonstration of covalent attachment of Au is challenging. XPS and AFM provide indirect evidence of the covalent link between Au and SH groups.

#### 5. CONTROL OF DEGREE OF ORIENTATION OF PURPLE MEMBRANE FILMS USING KELVIN PROBE FORCE MICROSCOPY TECHNIQUE

The degree of orientation achieved upon the preparation of highly oriented monolayers of bR-containing PMs and QD-PM hybrid materials should be carefully controlled if an efficient photovoltaic device needs to be prepared. Our suggested approach to the quality control of flame-annealed atomic-smooth gold coating with PMs is based on the Kelvin probe force microscopy (KPFM) technique. KPFM allows the distribution of the surface potential of a sample to be plotted with a high spatial resolution simultaneously with its topographic imaging<sup>37</sup> and was proved to be efficient for studying different photosensitive membranes,<sup>38</sup> including PMs.<sup>39</sup>

The procedure of the quality control of PMs gold coating uses the setup shown in Figure 4 and combines surface probe microscopy (SPM, allowing for KPFM) and an inverted optical microscope. The inverted optical microscope is used for light irradiation, through a 20 $\times$  objective; the light spot is localized precisely under the metallized SPM probe serving for measuring the surface potential and obtaining a topographic image.

The main criteria of the quality of the gold surface coating with the PMs are its high density, homogeneity, and high degree of orientation of the sedimented PMs. KPFM allows all of these parameters to be controlled simultaneously (Figure 4). The coating density and homogeneity can be estimated using the statistical methods of roughness analysis.<sup>41</sup> Ideally, the sample surface should be extremely smooth, with RMS  $\sim 1$  Å and the maximum height variation corresponding to the only narrow peak of the roughness histogram; its value should be  $\sim 5$  nm, that is, approximately equal to the PM height. In this ideal case, there should be only two types of smooth plains differing in height by  $\sim 5$  nm: the area of the lower plain (the Au surface) is substantially smaller compared with the higher one (the PM surface).

The degree of PM orientation on the gold surface and KPFM images obtained in the dark and under illumination should be statistically compared. A halogen lamp can be used as a source of light, which is passed through a 495 nm long pass filter; the resulting incident illumination is  $77 \text{ W/cm}^{-2}$ .<sup>40</sup> The change in the bR surface potential upon illumination is caused by its structural changes. It is known that upon illumination the

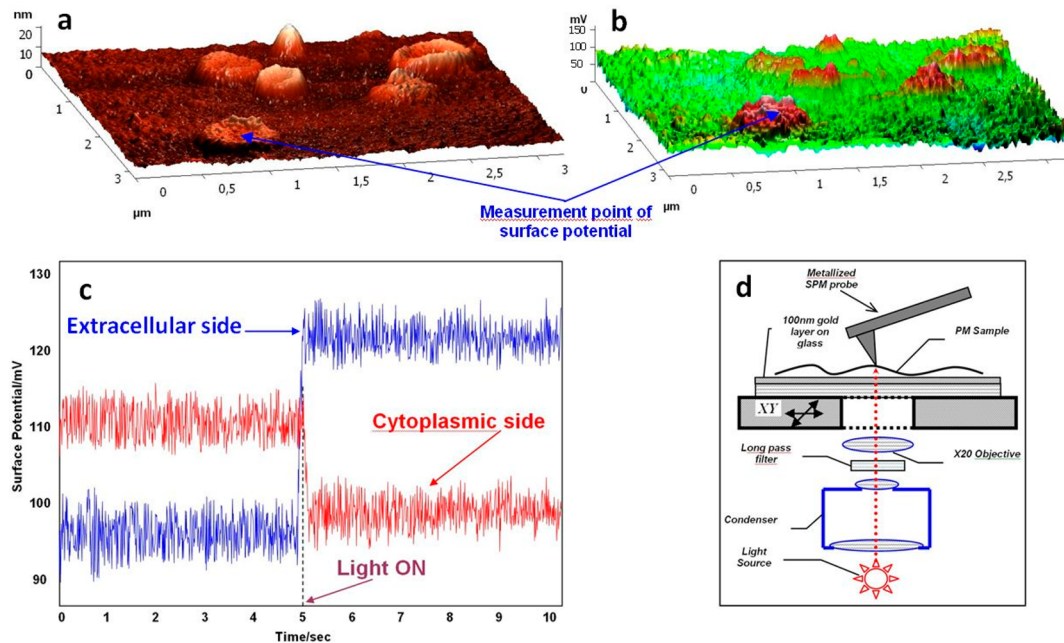


**Figure 4.** Control of the purple membrane film density, homogeneity, and degree of orientation on the gold surface using the simultaneous atomic force microscopy and Kelvin probe force microscopy technique. Simultaneous atomic force microscopy (a) and Kelvin probe force microscopy (b) imaging of the purple membrane adsorbed on the gold surface is demonstrated. (c) Surface potential measurement of the purple membrane fragment in the dark and upon illumination. (d) Experimental setup.

surface potential of the cytoplasmic PM surface decreases by  $\sim 10$  mV and that of the external surface increases by  $\sim 15$  mV,<sup>40</sup> which is clearly seen in our experiment shown in Figure 4. This behavior of the surface potential is explained by accumulation of protons on the external PM surface, where protons are injected as a result of the Schiff's base deprotonation upon the transition of the irradiated bR into the M form. The procedure of the quality control of the gold surface coating and degree of PM orientation should be performed under the conditions of controlled humidity (50–70%); the obtained highly oriented films may be further dried and used in liquid-free BSSC-based devices.

The main criteria of the quality of gold surface coating with the PM are the film high density and homogeneity (measured using AFM) and a high degree of orientation of the sedimented PMs (evaluated using KPFM). KPFM measures the changes in the surface potential upon illumination, which are opposite in sign for PM orientation to the gold surface with its cytoplasmic or external side of the membrane.

## 6. CONCLUSIONS

If the efficiency of the proposed solid-state photovoltaic device is to be increased to practical levels, further development is needed, such as introducing light-trapping structures to boost the light-harvesting capacity of the molecular photoreceptors on the flat device surface, achievement of high orientation of active energy transferring monolayers of hybrid materials on the gold surface, and the possibility to control the structure, degree of orientation, and function of engineered photoactive monolayers. Here we study a novel nanobiohybrid material with advanced photonic and photovoltaic properties based on the unique optical characteristics of colloidal fluorescent QDs, the photovoltaic properties of bR, and the state-of-the-art nanobioengineering approaches, permitting spatial and optimal

coupling together with control of nano- and biocomponents in hybrid material.

Although several biomolecules could be considered for solar cell applications, bR has received considerable attention because of its long-term stability against thermal, chemical, and photochemical degradation and its desirable electric and photochromic properties, along with the ability to maintain its biological activity for many years. A specially designed mutant of bR with an engineered Cys at position 247 is immobilized on a gold substrate with a strong covalent bond similar to Cys3 bR also immobilized on gold substrate.<sup>33</sup> A combined AFM-KPFM approach permits the quality of coating and degree of orientation of the sedimented PMs and hybrid materials on gold surface to be controlled, thus providing the next step toward development of bR-based BSSC devices with advanced photovoltaic properties.

Some FRET efficiencies of the QD/bR systems exceed the values given by classical FRET theory formulated by Forster.<sup>18</sup> We now have a new theory<sup>19</sup> explaining these discrepancies. However, our current treatment of vibration is still simple and could benefit from further studies and refinements. In fact, it is well understood that proteins are not static structures<sup>41,42</sup> but rather dynamic bodies that exhibit motions over a wide range of time and length scales. These motions are especially relevant to optimizing energy transfer from bR to metal-oxide surfaces through the two mechanisms central to the function of this biosensitized cell. First, bR proton pumping mechanism is predicated on motions throughout the  $\alpha$ -helical structures initiated by the retinal cis-trans conformation transitions induced by photon absorptions.<sup>43,44</sup> FRET transfer efficiencies are highly dependent on the distances from acceptor and donor up to 15 nm. Within this spatial range, energy-transfer efficiencies are inversely proportional to the sixth power of the distance between energy donor and acceptor, and the variations in acceptor/donor distances due to perturbations in

protein structure fall within these spatial scales<sup>45,46</sup> and are hypothesized in this paper to play a significant role in determining charge-transfer efficiency from the excited protein to metal oxide collector. In the case of the proposed QD enhanced biosolar cell, bR is covalently attached to inorganic semiconductor surfaces. The effects of the anisotropic forces normally found at interfaces on protein dynamics are not yet well understood; several studies have linked protein flexibility with solvent interactions.<sup>47–49</sup> Furthermore, Chin and Somasundaran have reported increased enzyme performance in the presence of surfactant aggregates via enhanced flexibility in the protein structures.<sup>50</sup>

## ■ ASSOCIATED CONTENT

### Supporting Information

This material is available free of charge via the Internet at <http://pubs.acs.org>.

## ■ AUTHOR INFORMATION

### Notes

The authors declare no competing financial interest.

## ■ ACKNOWLEDGMENTS

We thank Dr. C. N. Chinnasamy (Electron Energy Corporation) and Dr. U. Tylus Latosiewicz (Northeastern University) for discussions and Dr. N. Bouchonville (Université de Reims Champagne-Ardenne) for AFM measurements. V.R. acknowledges partial support from NIH, NSF, Rothschild Foundation, and Harvard Medical School. B.B. is supported by the U.S. Department of Energy, Office of Science, Basic Energy Sciences contract no. DE-FG02-07ER46352, and he has benefited from Northeastern University's Advanced Scientific Computation Center (ASCC), theory support at the Advanced Light Source, Berkeley, and the allocation of supercomputer time at NERSC through grant no. DE-AC02-05CH11231. IN and A.S. acknowledge support of the European Commission through the FP7 Cooperation Program NAMDIATREAM (grant no. NMP-2009-4.0-3-246479) and Ministry of Higher Education and Science of the Russian Federation (grant no. 11.G34.31.0050). M.M. and I.N. acknowledge partial support from DRRT, Region Champagne Ardenne and FEDER funding through HYNNOV program and Nano'Mat Platform. P.S. acknowledges support from the National Science Foundation Industry/University cooperative Research Center. Research in the EP laboratory has been supported by the Ministerio de Ciencia e Innovación and FEDER (Fondo Europeo de Desarrollo Regional) grant BFU2012-40137-C02-01. The authors would like to thank Neus Ontiveros for skillful technical help. This work is dedicated to Varun.

## ■ REFERENCES

- (1) Gratzel, M. Photoelectrochemical Cells. *Nature* **2001**, *414*, 338–344.
- (2) Gratzel, M. Applied Physics: Solar Cells to Dye For. *Nature* **2003**, *421*, 586–587.
- (3) Thavasi, V.; Renugopalakrishnan, V.; Jose, R.; Ramakrishna, S. Controlled Electron Injection and Transport at Materials Interfaces in Dye Sensitized Solar Cells. *Mater. Sci. Eng., R* **2009**, *63*, 81–99.
- (4) McFarland, E. W.; Tang, J. A Photovoltaic Device Structure Based on Internal Electron Emission. *Nature* **2003**, *421*, 616–618.
- (5) Thavasi, V.; Lazarova, T.; Filipek, S.; Kolinski, M.; Querol, E.; Kumar, A.; Ramakrishna, S.; Padros, E.; Renugopalakrishnan, V. Study on the Feasibility of Bacteriorhodopsin as Bio-Photosensitizer in

Excitonic Solar Cell: A First Report. *J. Nanosci. Nanotechnol.* **2009**, *9*, 1679–1687.

(6) Khizroev, S.; Ikkawi, R.; Amos, N.; Chomko, R.; Renugopalakrishnan, V.; Haddon, R.; Litvinov, D. Protein-Based Disk Recording at Areal Densities Beyond 10 Terabits/in.2. *MRS Bull.* **2008**, *33*, 864–871.

(7) Spudich, E. N.; Ozorowski, G.; Schow, E. V.; Tobias, D. J.; Spudich, J. L.; Luecke, H. A Transporter Converted Into a Sensor, a Phototaxis Signaling Mutant of Bacteriorhodopsin at 3.0 Å. *Mol. Biol.* **2012**, *415*, 455–463.

(8) Lazarova, T.; Mlynarczyk, K.; Filipek, S.; Kolinski, M.; Wassenaar, T.; Querol Murillo, E.; Renugopalakrishnan, V.; Viswanathan, S.; Padros, E. The Effect of Triple Glutamic Mutations E9Q/E194Q/E204Q on the Structural Stability of Bacteriorhodopsin. *FEBS J.* **2013**, *281*, 1181–1195.

(9) Brown, L. S.; Sasaki, J.; Kandori, H.; Maeda, A.; Needleman, R.; Lanyi, J. K. Glutamic Acid 204 is the Terminal Proton Release Group at the Extracellular Surface of Bacteriorhodopsin. *J. Biol. Chem.* **1995**, *270*, 27122–27126.

(10) Weilmeier, M. K.; Rippard, W. H.; Buhrman, R. A. Ballistic Electron Transport Through Au(111)/Si(111) and Au(111)/Si(100) Interfaces. *Phys. Rev. B* **1999**, *59*, R2521–R2524.

(11) Mukherjee, S.; Renugopalakrishnan, V.; Barbiellini, B.; Viswanathan, S.; Chin, M.; Somasundaran, P. The Scientific Symposium, Materials Challenges for Clean Energy in the New Millennium. *Mater. Today* **2009**, *12*, 62–63.

(12) Bertoncello, P.; Nicolini, D.; Paternolfi, C.; Bavastrello, V.; Nicolini, C. Bacteriorhodopsin-Based Langmuir-Schaefer Films for Solar Energy Capture. *IEEE Trans. Nanobiosci.* **2003**, *2*, 124–132.

(13) Das, R.; Kiley, P. J.; Segal, M.; Norville, J.; Yu, A. A.; Wang, L.; Trammell, S. A.; Reddick, L. E.; Kumar, R.; Stellacci, F.; et al. Integration of Photosynthetic Protein Molecular Complexes in Solid-State Electronic Devices. *Nano Lett.* **2004**, *4*, 1079–1083.

(14) Samokhvalov, P.; Artemyev, M.; Nabiev, I. Basic Principles and Current Trends in Colloidal Synthesis of Highly Luminescent Semiconductor Nanocrystals. *Chem.—Eur. J.* **2013**, *19*, 1534–1546.

(15) Li, R.; Li, C. M.; Bao, H.; Bao, Q.; Lee, V. S. Stationary Current Generated from Photocycle of a Hybrid Bacteriorhodopsin/quantum Dot Bionanosystem. *Appl. Phys. Lett.* **2007**, *91*, 223901–223901–3.

(16) Rakovich, A.; Sukhanova, A.; Bouchonville, N.; Lukashev, E.; Oleinikov, V.; Artemyev, M.; Lesnyak, V.; Gaponik, N.; Molinari, M.; Troyon, M.; et al. Resonance Energy Transfer Improves the Biological Function of Bacteriorhodopsin Within a Hybrid Material Built from Purple Membranes and Semiconductor Quantum Dots. *Nano Lett.* **2010**, *10*, 2640–2648.

(17) Bouchonville, N.; Molinari, M.; Sukhanova, A.; Artemyev, M.; Oleinikov, V. A.; Troyon, M.; Nabiev, I. Charge-Controlled Assembling of Bacteriorhodopsin and Semiconductor Quantum Dots for Fluorescence Resonance Energy Transfer-Based Nanophotonic Applications. *Appl. Phys. Lett.* **2011**, *98*, 013703.

(18) Bouchonville, N.; Cigne, A. L.; Sukhanova, A.; Molinari, M.; Nabiev, I. Nano-Biophotonic Hybrid Materials with Controlled FRET Efficiency Engineered from Quantum Dots and Bacteriorhodopsin. *Laser Phys. Lett.* **2013**, *10*, 085901.

(19) King, C.; Barbiellini, B.; Moser, D.; Renugopalakrishnan, V. Exactly Soluble Model of Resonant Energy Transfer Between Molecules. *Phys. Rev. B* **2012**, *85*, 125106.

(20) Barbiellini, B.; Platzman, P. M. The Healing Mechanism for Excited Molecules Near Metallic Surfaces. *New J. Phys.* **2006**, *8*, 20.

(21) Mukherjee, S.; Nadesalingam, M. P.; Guagliardo, P.; Sergeant, A. D.; Barbiellini, B.; Williams, J. F.; Fazleev, N. G.; Weiss, A. H. Auger-Mediated Sticking of Positrons to Surfaces: Evidence for a Single-Step Transition from a Scattering State to a Surface Image Potential Bound State. *Phys. Rev. Lett.* **2010**, *104*, 247403.

(22) Renugopalakrishnan, V.; Garduno-Juarez, R.; Narasimhan, G.; Verma, C. S.; Wei, X. L. P. Rational Design of Thermally Stable Proteins: Relevance to Bionanotechnology. *J. Nanosci. Nanotechnol.* **2005**, *5*, 1759–1767.

- (23) Kelzenberg, M. D.; Boettcher, S. W.; Petykiewicz, J. A.; Turner-Evans, D. B.; Putnam, M. C.; Warren, E. L.; Spurgeon, J. M.; Briggs, R. M.; Lewis, N. S.; Atwater, H. A. Enhanced Absorption and Carrier Collection in Si Wire Arrays for Photovoltaic Applications. *Nat. Mater.* **2010**, *9*, 239–244.
- (24) Shankar, K.; Basham, J. I.; Allam, N. K.; Varghese, O. K.; Mor, G. K.; Feng, X.; Paulose, M.; Seabold, J. A.; Choi, K.-S.; Grimes, C. A. Recent Advances in the Use of TiO<sub>2</sub> Nanotube and Nanowire Arrays for Oxidative Photoelectrochemistry. *J. Phys. Chem. C* **2009**, *113*, 6327–6359.
- (25) Kim, C. H.; Thompson, L. T. Deactivation of Au/CeO<sub>x</sub> Water Gas Shift Catalysts. *J. Catal.* **2005**, *230*, 66–74.
- (26) Kanai, Y.; Neaton, J. B.; Grossman, J. C. Theory and Simulation of Nanostructured Materials for Photovoltaic Applications. *Comput. Sci. Eng.* **2010**, *12*, 18–27.
- (27) Harju, A.; Barbiellini, B.; Siljamäki, S.; Nieminen, R. M.; Ortiz, G. Stochastic Gradient Approximation: An Efficient Method to Optimize Many-Body Wave Functions. *Phys. Rev. Lett.* **1997**, *79*, 1173–1177.
- (28) Xingyu, G.; Viswanathan, S. N.; Chang, C.-W.; Barbiellini, B.; Budil, D. E.; Renugopalakrishnan, V. Spectroscopic Determination of HOMO and LUMO Energies of Retinal in Bacteriorhodopsin for Solar Cell Applications. *Biophys. J.* **2010**, *98*, 172.
- (29) Eijt, S. W. H.; Veen, A.; van Schut, H.; Mijnarends, P. E.; Denison, A. B.; Barbiellini, B.; Bansil, A. Study of Colloidal Quantum Dot Surfaces Using an Innovative Thin-Film Positron 2D-ACAR Method. *Nat. Mater.* **2006**, *5*, 23.
- (30) Eijt, S. W. H.; Mijnarends, P. E.; Schaarenburg, L. C.; van Houtepen, A. J.; Vanmaekelbergh, D.; Barbiellini, B.; Bansil, A. Electronic Coupling of Colloidal CdSe Nanocrystals Monitored by Thin-Film Positron-Electron Momentum Density Methods. *Appl. Phys. Lett.* **2009**, *94*, 091908.
- (31) Chai, L.; Al-Sawai, W.; Gao, Y.; Houtepen, A. J.; Mijnarends, P. E.; Barbiellini, B.; Schut, H.; van Schaarenburg, L. C.; van Huis, M. A.; Ravelli, L.; et al. Surfaces of Colloidal PbSe Nanocrystals Probed by Thin-Film Positron Annihilation Spectroscopy. *APL Mater.* **2013**, *1*, 022111.
- (32) Somasundaran, P.; Chin, M.; Latosiewicz, U. T.; Tuller, H. L.; Barbiellini, B.; Renugopalakrishnan, V. Nanoscience and Engineering for Robust Biosolar Cells. In *Bionanotechnology II: Global Prospects*; Reisner, D., Ed.; CRC Press: Boca Raton, FL, 2011.
- (33) Zaitsev, S. Y.; Solovyeva, D. O.; Nabiev, I. Thin Films and Assemblies of Photosensitive Membrane Proteins and Colloidal Nanocrystals for Engineering of Hybrid Materials with Advanced Properties. *Adv. Colloid Interface Sci.* **2012**, *183–184*, 14–29.
- (34) Sanz, C.; Lazarova, T.; Sepulcre, F.; González-Moreno, R.; Bourdelande, J. L.; Querol, E.; Padrós, E. Opening the Schiff Base Moiety of Bacteriorhodopsin by Mutation of the Four Extracellular Glu Side Chains. *FEBS Lett.* **1999**, *456*, 191–195.
- (35) Ferrando, E.; Schweiger, U.; Oesterhelt, D. Homologous Bacterio-Opsin-Encoding Gene Expression via Site-Specific Vector Integration. *Gene* **1993**, *125*, 41–47.
- (36) Oesterhelt, D.; Stoeckenius, W. Isolation of the Cell Membrane of Halobacterium Halobium and Its Fractionation Into Red and Purple Membrane. *Methods Enzymol.* **1974**, *31*, 667–678.
- (37) Jacobs, H. O.; Leuchtmann, P.; Homan, O. J.; Stemmer, A. Resolution and Contrast in Kelvin Probe Force Microscopy. *J. Appl. Phys.* **1998**, *84*, 1168–1173.
- (38) Lee, I.; Greenbaum, E.; Budy, S.; Hillebrecht, J. R.; Birge, R. R.; Stuart, J. Photoinduced Surface Potential Change of Bacteriorhodopsin Mutant D96N Measured by Scanning Surface Potential Microscopy. *J. Phys. Chem. B* **2006**, *110*, 10982–10990.
- (39) Knapp, H. F.; Mesquida, P.; Stemmer, A. Imaging the Surface Potential of Active Purple Membrane. *Surf. Interface Anal.* **2002**, *33*, 108–112.
- (40) Patil, A. V.; Premaraban, T.; Berthoumieu, O.; Watts, A.; Davis, J. J. Engineered Bacteriorhodopsin: A Molecular Scale Potential Switch. *Chem.—Eur. J.* **2012**, *18*, 5632–5636.
- (41) Koshland, D. Conformational Changes: How Small Is Big Enough? *Nat. Med.* **1998**, *4*, 1112–1114.
- (42) Dobbins, S. E.; Lesk, V.; Sternberg, M. J. E. Insights Into Protein Flexibility: The Relationship Between Normal Modes and Conformational Change Upon Protein-Protein Docking. *Proc. Natl. Acad. Sci. U.S.A.* **2008**, *105*, 10390–10395.
- (43) McDermott, A. E.; Thompson, L. K.; Winkel, C.; Farrar, M. R.; Pelletier, S.; Lugtenburg, J.; Herzfeld, J.; Griffin, R. G. Mechanism of Proton Pumping in Bacteriorhodopsin by Solid-State NMR: The Protonation State of Tyrosine in the Light-Adapted and M States. *Biochemistry* **1991**, *30*, 8366–8371.
- (44) Edholm, O.; Berger, O.; Jähnig, F. Structure and Fluctuations of Bacteriorhodopsin in the Purple Membrane: A Molecular Dynamics Study. *J. Mol. Biol.* **1995**, *250*, 94–111.
- (45) Lee, B. Calculation of Volume Fluctuation for Globular Protein Models. *Proc. Natl. Acad. Sci. U. S. A.* **1983**, *80*, 622–626.
- (46) Paci, E.; Marchi, M. Constant-Pressure Molecular Dynamics Techniques Applied to Complex Molecular Systems and Solvated Proteins. *J. Phys. Chem.* **1996**, *100*, 4314–4322.
- (47) Broos, J.; Visser, A. J. W. G.; Engbersen, J. F. J.; Verboom, W.; van Hoek, A.; Reinoudt, D. N. Flexibility of Enzymes Suspended in Organic Solvents Probed by Time-Resolved Fluorescence Anisotropy. Evidence That Enzyme Activity and Enantioselectivity Are Directly Related to Enzyme Flexibility. *J. Am. Chem. Soc.* **1995**, *117*, 12657–12663.
- (48) Affleck, R.; Xu, Z. F.; Suzawa, V.; Focht, K.; Clark, D. S.; Dordick, J. S. Enzymatic Catalysis and Dynamics in Low-Water Environments. *Proc. Natl. Acad. Sci. U. S. A.* **1992**, *89*, 1100–1104.
- (49) Yang, L.; Dordick, J. S.; Garde, S. Hydration of Enzyme in Nonaqueous Media Is Consistent with Solvent Dependence of Its Activity. *Biophys. J.* **2004**, *87*, 812–821.
- (50) Chin, M.; Somasundaran, P. Enzyme Activity and Structural Dynamics Linked to Micelle Formation: A Fluorescence Anisotropy and ESR Study. *Photochem. Photobiol.* **2014**, *90*, 455–462.